EPJ manuscript No.
(will be inserted by the editor)

Feasibility of a storage ring for polar molecules in strong-field-seeking states

Hiroshi Nishimura[1], Glen Lambertson[2], Juris G. Kalnins[2] and Harvey Gould[2]

Mail Stop [1]80-101, [2]71-259, Lawrence Berkeley National Laboratory, University of California, Berkeley, California 94720

Received: date / Revised version: date

Abstract. We show, through modeling and simulation, that it is feasible to construct a storage ring that will store dense bunches of strong-field-seeking polar molecules at 30 m/s (kinetic energy of 2K) and hold them, for several minutes, against losses due to defocusing, oscillations, and diffusion. The ring, 3 m in diameter, has straight sections that afford access to the stored molecules and a lattice structure that may be adapted for evaporative cooling. Simulation is done using a newly-developed code that tracks the particles, in time, through 400 turns; it accounts for longitudinal velocity changes as a function of external electric field, focusing and deflection nonlinearities, and the effects of gravity. An injector, decelerator, and source are included and intensities are calculated.

PACS. 2 9.20 Dh, 41.75.Lx, 33.80.Ps, 39.90.+d, 33.55.Be

1 Introduction

To date, all gaseous quantum condensates have been produced by evaporative cooling of confined atoms. Confinement is necessary to thermally isolate the particles from the warmer environment and long confinement times are necessary because the evaporative cooling process can take tens of seconds.

Strong magnetic field gradients have been used to confine neutral paramagnetic molecules [1] and electric-field gradients have been used to confine neutral polar molecules in electrostatic traps [2] and in toroidal storage rings [3,4]. In addition, polar molecule confinement in a synchrotron storage ring has been modeled [5].

All of these methods use molecules or atoms in weak-field-seeking states, whose binding energy decreases in the field. These states are not the lowest energy state and are therefore subject to collisional relaxation. In alkali atoms, the relaxation rates from the stretched hyperfine levels ($m_F = F$) is small. But in magnetically trapped paramagnetic molecules [6] and in electrically confined polar molecules [7–10], the relaxation rate can be large enough to prevent achieving the confinement time needed for evaporative cooling.

Collisional relaxation will be absent for polar molecules in their lowest rotational state. This ground state is strong-field-seeking, as are all rotational states in the limit of strong electric field. The technical challenges of storing molecules in a strong-field-seeking state have not been previously addressed. The major challenge is focusing these molecules because electrostatic lenses can focus strong-field-seeking molecules in only one transverse plane while defocusing in the other. Therefore alternating-gradient focusing is required.

For experiments on molecules in strong-field-seeking states, a storage ring has some useful features not generally found in traps. The ring has a beam geometry with field-free regions accessible to experiments, and it can simultaneously store many bunches of particles producing a large flux of molecules.

In this paper we show, by modeling and simulation, that it is feasible to construct a storage ring (Fig.1) that will store a symmetric-top molecule (methyl fluoride) in the $J = 0$ state, at a kinetic energy of 2 K (30 m/s), and by extension other molecules and velocities. In the storage ring, bunching electrodes hold the molecules in a string of short bunches. The molecules are calculated to be stable against losses due to defocusing, oscillations, and diffusion for over two minutes. We also model a decelerator for slowing the molecules to 30 m/s, and an injector for loading the storage ring.

A storage ring in which the density of the molecules in a bunch is allowed to vary around the ring, can provide a mechanism for evaporative cooling. Regions of high density speed the thermalization of the molecules. In regions of low density the molecules can become spatially separated due to their velocity spread allowing the hottest molecules to be removed.

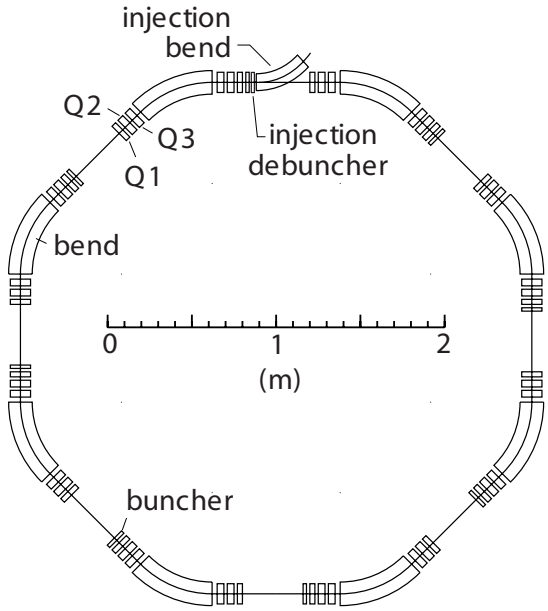

Fig. 1. Layout of the storage ring. Each octant contains a buncher and a pair of alternating-gradient focusing triplets to match the beam traversing from the straight sections to the bend sections. A bend section contains combined bend and alternating gradient focusing elements. The focusing and bend elements have time-independent electric fields. An injection line is located in one of the straight sections

2 Forces Due to Electric Field Gradients

2.1 Focusing and Deflection Using Multipole Fields

A brief description of focusing and deflecting a beam of molecules using electrostatic multipole fields is given below. Additional details of beam transport and focusing of molecules in strong-field-seeking states, with specific application to methyl fluoride in the $J = 0$ state, may be found in Kalnins et al. [11].

The guide field in a storage ring for molecules in strong-field-seeking states must provide all the functions, such as focusing, bending, and bunching, that are used in a ring for charged particles but with forces that arise from gradients of the magnitude of the electric field.

In a pure quadrupole or sextupole field, the total electric field increases radially and the force on a molecule, in a strong-field-seeking state, is away from the centerline in all transverse directions. Therefore a dipole component must be added to remove the double-defocusing, and obtain focusing in one transverse direction while still defocusing in the other. The force on a molecule is given by the gradient of its Stark potential energy, $W(E)$:

$$\boldsymbol{F} = -\nabla W(E) = -\frac{dW}{dE}\nabla E \tag{1}$$

where E is the magnitude of an external field.

The Stark energy of the molecular level is in general a nonlinear function and is described for methyl fluoride in the $J = 0$ rotational state in Ref. [11]. In the limit of large E, $W(E) \rightarrow -d_e E$ where d_e is the molecule's electric dipole moment.

The transverse (x horizontal, y vertical) electric multipole potential used to bend and focus a molecule is:

$$\Psi = E_0[y + A_2 xy + A_3(x^2 y - \frac{1}{3}y^3)] \tag{2}$$

where E_0 is the dipole field strength, and A_2 and A_3 are the relative quadrupole and sextupole component strengths.

For the Stark energy in the high-field limit, the forces to second order are:

$$\begin{aligned} F_x &\rightarrow d_e E_0[A_2 + 2A_3 x - \frac{1}{2}(A_2^3 - 4A_2 A_3)y^2] \\ F_y &\rightarrow d_e E_0[(A_2^2 - 2A_3)y - (A_2^3 - 4A_2 A_3)xy] \end{aligned} \tag{3}$$

We see that a combined dipole and sextupole (A_3) field lens will focus in one plane, while defocusing in the other. To deflect the molecule we must add a quadrupole (A_2) component. This also defocuses the beam in the y direction and stronger sextupole (A_3) strengths are needed [12].

To obtain net focusing in both transverse planes, the lenses are arranged in a sequence with gradients alternating in sign ($A_3 < 0$ for x-focusing and $A_3 > 0$ for y-focusing).

2.2 Other Effects

When a molecule in a strong-field-seeking state enters the field of an electrode pair it is accelerated longitudinally, and upon exiting the field it is decelerated. Also, the fringing field is stronger away from the midplane and this causes a net defocusing force in the direction of the electric field. Between successive sets of electrodes, this unwanted defocusing is reduced if the dipole fields are of the same polarity and strength.

Longitudinal bunching, as in a charged-particle ring, requires a pulsed field. The field is ramped in a sawtooth or sine-wave form and the time-dependent acceleration is the net difference between the fields when entering and when exiting.

The effect of gravity is small but not negligible for 30 m/s molecules in this ring. The vertical orbit will be distorted and an orbit correction must be applied.

2.3 Equations of Motion

The equations of motion of a molecule in the ring are obtained from the Hamiltonian:

$$H = H_0 + W(E) - gy \tag{4}$$

where $W(E)$ is the Stark energy, g is the acceleration due to gravity, and H_0 is the kinetic energy which in a bend region is:

$$H_0 = \frac{1}{2m}(P_x^2 + P_y^2 + \frac{P_\theta^2}{(\rho + x)^2}) \tag{5}$$

where P_x and P_y are the transverse momenta, P_θ is the angular momentum and ρ is the bend radius. In straight sections the last term is replaced by the square of the longitudinal momentum, ${P_z}^2$.

The longitudinal variation of the Stark energy at the ends of electrodes (treated here as a step function) adds or subtracts from the kinetic energy, the change in longitudinal velocity being about $\pm 10\%$.

Vertical defocusing in a fringe field is derived from the longitudinal variation of the field on the midplane and to lowest order is:

$$(F_y)_{fringe} = -\frac{dW}{dE}\ [\frac{1}{E_y}(\frac{\partial E_y}{\partial z})^2 - \frac{\partial^2 E_y}{\partial z^2}]\ y \qquad (6)$$

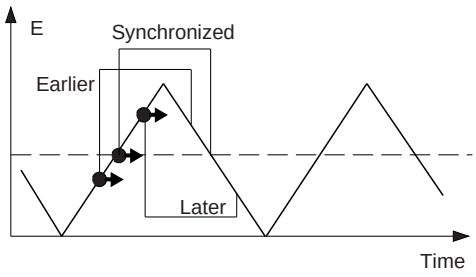

Fig. 2. A molecule at the bunch center enters and exits the buncher when the field is the same and receives no net acceleration. For a molecule that arrives later, the entering field is stronger than at its exit; it is accelerated and it then drifts downstream toward the bunch center.

3 Storage Ring Design

3.1 Molecule and Energy

The principles and techniques we use apply to all polar molecules in strong-field-seeking states. We choose methyl fluoride (CH_3F) as our reference molecule because it is a nearly symmetric rotor with a large electric dipole moment of $d_e = 6.2 \times 10^{-30}$ C-m (1.84 D). It has a moderate rotational constant of $B = 0.88$ cm^{-1} and a simple level structure with a $J = K = 0$ rotational ground state. The rotational constant is large enough to limit the number of rotational levels populated in the beam from a jet-source but still small enough to allow for a large Stark effect at moderate electric fields. Methyl fluoride is also a gas at room temperature.

The velocity of 30 m/s (kinetic energy of about 2K) is low enough to make for a compact ring, yet keep small the effects of gravity.

3.2 Ring Lattice

Long straight regions free of focusing electrodes make the stored beam accessible for experiments and give space for injection and extraction. Molecules, in order to drift through the straight section without loss, must have only small divergences and therefore a large beam width. In a bending region, we need strong deflecting forces to minimize the bend radius for overall compactness. These strong forces call for a small beam width to avoid nonlinearities. To make the transition (match) from straight sections to arc sections, triplets (Q1, Q2, Q3) of focusing lenses are placed at the ends of the straight sections, as shown in Fig. 1.

In each of the eight bend regions, there are five electrode pairs; each has a combined dipole and quadrupole field to provide the strong deflecting force. To this is added a sextupole component, the gradient of which alternates in sign.

The electrode parameters are given in Table 1 where Q are focusing elements and BF and BD are combined bend and focusing elements. Each arc is a series of BF and BD elements: $\frac{1}{2}$BF+BD+BF+BD+$\frac{1}{2}$BF.

In this sequence of lenses with alternating gradients, the molecules execute oscillatory transverse motions. The parameters of BF and BD are chosen such that the phases of these horizontal and vertical motions each advance through an angle of 2π in each octant of arc. The parameters of Q1, Q2 and Q3 are varied to find values that produce large dynamic aperture and momentum acceptance. The decapole coefficient, A_5 of Q2, which adds the term $E_0 A_5(x^4 y - 2x^2 y^2 + \frac{1}{5}y^5)$ to the potential Eq(2), is introduced to reduce the nonlinearity of Q2 focusing where the beam is at it's largest. For longitudinal confinement with many short bunches, we use eight bunchers in the ring; each has a short uniform field that is pulsed in time as illustrated in Fig. 2.

Molecules with different energies have their closed orbits radially separated in the arcs and perhaps elsewhere in the ring. If this dispersion of orbits is present at a buncher, the energy change from the buncher produces a shift in the orbit and an increment in the radial oscillation. This is called synchro-betatron coupling and to avoid growth of radial oscillation amplitude, the dispersion of orbits must be made zero at the bunchers. With the phases of the vertical and horizontal motions advancing through an angle of 2π in each octant, as noted above, the dispersion becomes zero at all eight buncher locations.

Table 1. Parameters of Storage Ring Electrodes

	Eo (MV/m)	L (cm)	A_2 (m^{-2})	A_3 (m^{-3})	A_5 (m^{-5})
Q1	3.0	3.34	0	2000	0
Q2	4.0	3.71	0	-2000	-1.28×10^6
Q3	4.0	2.85	0	2000	0
BF	7.85	4.00	-10.55	-2296	0
BD	7.85	4.00	-10.55	2343	0

3.3 Numerical Modeling and Simulation

The lattice parameters (Table 1) are found by numerical calculations using a newly-developed simulation code that

tracks the particles in time (rather than in longitudinal position) to account for the longitudinal velocity changes as a function of the external field. The tracking code includes the effects of nonlinearities, gravity and the longitudinal kick at the bunchers. The effect of each fringe field (Eq. 6) in every element has been integrated and replaced by a vertically defocusing thin lens. The parameters in Table 1 result in the ring performance listed in Table. 2 and shown in Figures 3 and 4.

Table 2. Ring Parameters

Parameter	Value
Circumference (m)	9.850
Circulation period (s)	0.3121
Velocity in free space (m/s)	30.0
Symmetry of the ring	8
Bending radius (m)	0.60
Long straight section (m)	0.40
Beta function* β_x (m)	0.274
β_y (m)	0.596
Dispersion* η_x (m)	0.0
Betatron tune ν_x	13.368
ν_y	10.398
Dynamic aperture* a_x (mm)	$\pm$1.75
a_y (mm)	$\pm$3.50
Acceptance ϵ_x (mm - mr)	11
ϵ_y (mm - mr)	21
Momentum acceptance (%)	$\pm$1.2
Number of longitudinal buckets	203

*At the center of straight sections

The beta functions and the horizontal dispersion are shown in Fig. 3b. Small beta functions in the bends produce a smaller beam profile, allowing the bend elements to be stronger and the beam to occupy the most linear region of the elements. The straight sections are designed to be free of horizontal dispersion to avoid synchro-beta coupling at the bunchers.

If uncorrected, the vertical closed orbit displacement caused by gravity is 2.6 mm and is large enough to cause loss of the circulating beam. The orbit is corrected by displacing Q2 by 0.24 mm downward to produce upward kicks. The resulting vertical orbit distortion shrinks to 0.26 mm as shown in Fig. 5 and is no longer a problem.

With this orbit correction, the dynamic aperture for 400 turns, at the center of a straight section, is about 2 mm by 3 mm half-width as shown in Fig. 4. This dynamic aperture corresponds to acceptances of 11 mm-mr horizontal and 21 mm-mr vertical, as listed in Table 2. The resulting beam size is shown in Fig. 3a. The momentum acceptance, calculated by the multi-particle tracking simulation, is $\pm$1.2% which is equivalent to an energy acceptance of $\pm$ 45 mK.

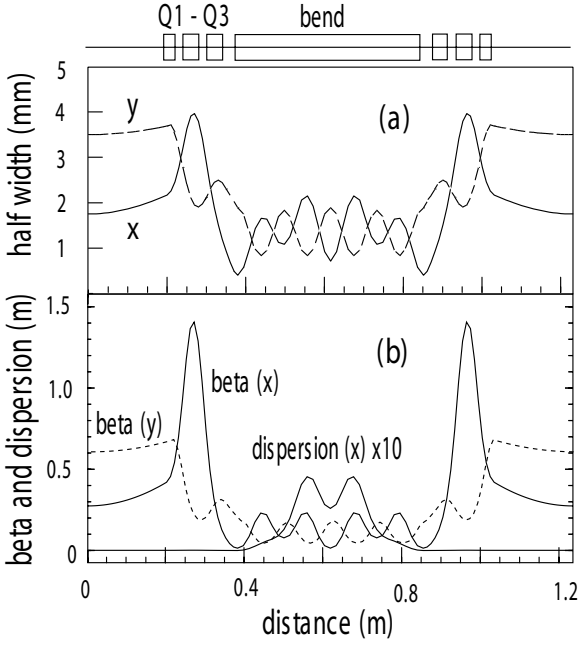

Fig. 3. Beam half-widths (a) and the beta functions and horizontal dispersion (b) in the storage ring. Beta is the distance in which the transverse (betatron) oscillation advances in phase by one radian. A schematic of the lattice is shown for location reference.

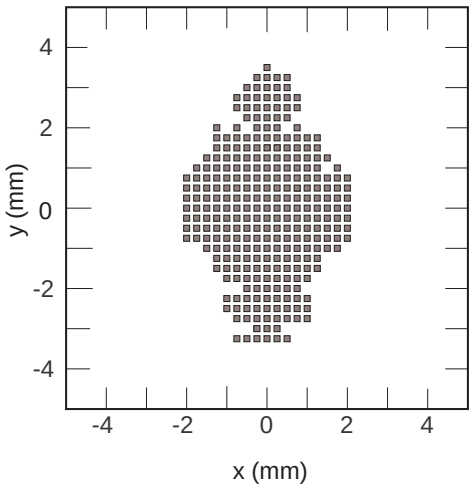

Fig. 4. Starting coordinates in the center of the straight section for the molecules that survive 400 turns. This defines the dynamic aperture.

4 Decelerated Beam

4.1 Decelerator

To reduce the velocity from the 310 m/s at the source to 30 m/s requires many stages of deceleration by pulsed electric fields in a long linear array. At each of the 139 decelerating stages, a bunch of molecules enters a set of

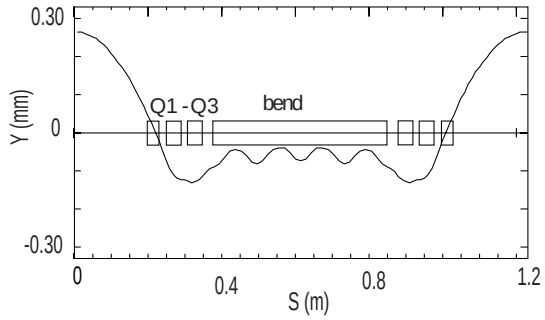

Fig. 5. Corrected vertical closed orbit displacement of the beam in the storage ring

Table 3. Parameters of the decelerator for injected beam

Parameter	Value
Velocity at source (m/s)	310
Velocity at exit (m/s)	30
Velocity spread at exit (%)	±2
Length of bunch at exit (mm)	10
Emittances at exit, x and y (mm-mr)	30
Electrode gap (mm)	7
Decelerating field at entrance (MV/m)	9
Decelerating field at exit (MV/m)	4.5
Length of last decel. electrode (mm)	24
Length of decelerator (m)	19.6
Number of decel. electrodes	139

parallel electrodes when the field is zero; the field pulses on and the molecules lose kinetic energy equal to $|W(E)|$ as they exit the electrodes.

Our decelerator design differs in almost every way from previous designs [13,14]. A decrease in the strength of the electric field while the bunch exits the electrodes provides longitudinal restoring action that prevents the bunch lengthening due to velocity spread [15]. The lengths of successive electrodes decreases as the velocity and spacing of the bunches decreases.

Interspersed between the pulsed parallel electrodes are alternating-gradient lenses to confine the molecules transversely. Their overall focusing action must be stronger in the plane of the electric fields to counter the defocusing from fringe fields. The major parameters of the decelerator are summarized in Table 3. Details of decelerator design will be published later.

4.2 Injector

To inject the beam, we need a bend electrode that can pulse on or off in the time between buckets in the ring. This allows us to store multiple (up to 203) bunches in the ring. The deflecting electrode (Fig.1) is part of a transport line that transforms the pulse leaving the decelerator to match the orientation of the transverse acceptances of the ring at the point of entry onto the closed orbit of the ring. The deflecting electrode is actually an array of bend electrodes with radius 0.6 m, similar to a bend section in the ring. A horizontal phase advance of 2π in this bend, avoids a net dispersal of molecules that are within the ±2 % velocity spread.

In passage along the line, the velocity spread of ±2% lengthens the bunch and a debuncher at the point of injection (Fig 1) brings 90% of the bunch within the ±1.2% longitudinal momentum acceptance of the ring.

4.3 Source and Intensity

We calculate the intensity based upon a pulsed jet source with 1% methyl fluoride seeded in xenon carrier gas, using the equations in Miller [16] and verified against seeded xenon jet source performance reported in the literature [3,4,17]. Xenon's high mass (133) produces much slower beams (310 m/s from a room-temperature reservoir) than do light carrier gases, resulting in a shorter (19.6 m) decelerator.

The bunch intensity is determined by the source flow rate, the $J = 0$ state population, velocity distribution and acceptances. A source orifice of 1 mm diameter and reservoir pressure of 6.56×10^4 Pa (500 Torr) will produce an intense cold beam with a peak intensity of 3×10^{19} molecules sr^{-1} s^{-1} with a longitudinal velocity spread of 7.2 m/s FWHM and less than 1% clusters. We estimate the methyl fluoride J = 0 rotational state fraction to be 30%. In an apparatus with a finite pumping speed, this peak intensity is possibly only with a pulsed jet source operating at a small duty cycle. The short widely-spaced beam pulses entering the decelerator (which become more closely spaced after deceleration) require less than a one percent jet source duty cycle for a 100 Hz pulse rate. This would allow all 203 buckets in the ring to be filled in 6.4 turns.

The fraction of the molecules accepted into each transverse direction of the storage ring is the ratio of the horizontal and vertical acceptances of the storage ring to the horizontal and vertical emittances of the source. When expressed as half-width times transverse velocity spread (units of m^2 s^{-1}), the ratio is independent of longitudinal velocity. If the beam from the source has ±0.5 mm spatial extent and ±1000 mr angular divergence, then the horizontal and vertical acceptances of the storage ring (Table 2) of 11 mm-mr and 21 mm-mr respectively, result in 8.66×10^{-6} of the molecules being transversely accepted.

The longitudinal velocity spread scales inversely as the square root of the velocity [18]. The ±2% velocity spread out of the decelerator (± 0.6 m/s) transforms to ±0.19 m/s velocity spread at the source and within this spread there will be 6.4 % of the jet-source molecules. The 10 mm bunch length in the storage ring scales as the square root of the velocity [18] becoming a 32 mm-long bunch at the source. Each bunch would then start with about 9.3×10^{14} molecules in the $J = 0$ state.

Combining these nunbers and acounting for the 90% acceptance of the storage ring from the injector yields an intensity of 5×10^8 molecules/bunch. Bunches could be injected into the storage ring singularly or in large numbers.

With a maximum of 203 stored bunches there would be nearly 1.0×10^{11} molecules circulating in the storage ring and a flux of 3.3×10^{11} molecules/s. Each bunch would have a density of about 4×10^{9} molecules/cm^3 in the long straight sections, and higher in the bends.

5 Acknowledgments

The authors acknowledge and thank Richard Gough and David Robin for their enthusiastic encouragement, and Swapan Chattopadhyay and Ying Wu for early contributions to the storage ring work. Work supported by the Director, Office of Science; Office of Basic Energy Sciences, and Office of High Energy and Nuclear Physics, U.S. Department of Energy, under Contract No. DE-AC03-76SF00098.

References

1. J. D. Weinstein, R. deCarvalho, T. Guillet, B. Friedrich and J.M. Doyle, Nature **395**, 148 (1998).
2. H.L. Bethlem, G. Berden, F.M.H. Crompvoets, R.T. Jongma, A.J.A. van Roij, and G. Meijer, Nature **406**, 491 (2000).
3. F.M.H. Crompvoets, H.L. Bethlem, R.T. Jongma, and G. Meijer, Nature **411**, 174 (2001).
4. F.M.H. Crompvoets, H.L. Bethlem, J. Küpper, A.J.A. van Roij and G. Meijer, Phys. Rev. A**69**, 063406 (2001).
5. H. Nishimura, G. Lambertson, J. G. Kalnins, and H. Gould, Rev. Sci. Instr. **43**, 3271 (2003).
6. A. Volpi and J.L. Bohn, Phys. Rev. A**65**, 052712 (2002).
7. J. L. Bohn, Phys. Rev. A**63**, 052714 (2001).
8. M. Kajita, T. Suzuki, H. Odashima, Y. Moriwaki, and M. Tachikawa, Jpn. J. Appl. Phys. **40**, L1260 (2001).
9. M. Kajita, Eur. Phys. J. D**20**, 55 (2002).
10. A.V Avdeenkov and J.L. Bohn, Phys. Rev. A**66**, 0052718 (2002).
11. J.G. Kalnins, G. Lambertson, and H. Gould, Rev. Sci. Instr. **73**, 2557 (2002).
12. H. Nishimura, G. Lambertson, J.G. Kalnins, and H. Gould, IEEE Proc. of PAC 2003, 1837 (2002).
13. H.L. Bethlem, A.J.A. van Roij, R.T. Jongma and G. Meijer, Phys. Rev. Lett. **88**, 133003 (2002).
14. M.R. Tarbutt, H.L. Bethlem, J.J. Hudson, V.L. Ryabov, V.A. Ryzhov, B.E. Sauer, G. Meijer, and E.A. Hinds, Phys. Rev. Lett. **92**, 173002 (2004).
15. J.A. Maddi, T.P. Dinneen, and H. Gould, Phys. Rev. A**60**, 3882 (1999).
16. D.R. Miller, in *Atomic and Molecular Beam Methods*, edited by G. Scoles (Oxford University Press, New York, 1988), Vol. 1, p. 14.
17. M. Gupta and D. Herschbach, J. Phys. Chem. **103**, 10670 (1999).
18. G. Lambertson, private communication, 2004.